# THE ROTATING NUCLEAR THOMAS–FERMI MODEL*,**

W.D. MYERS AND W.J. SWIATECKI

Nuclear Science Division, Lawrence Berkeley Laboratory
University of California, Berkeley, California 94720, USA

*(Received December 8, 1995)*

The Thomas–Fermi model of W.D. Myers and W.J. Swiatecki (*Nuclear Properties According to the Thomas–Fermi Model*, Lawrence Berkeley Laboratory preprint LBL-36557, December 1994, submitted to *Nucl. Phys. A*; *Table of Nuclear Masses According to the 1994 Thomas–Fermi Model*, Lawrence Berkeley Laboratory preprint LBL-36803, December 1994) is generalized by the addition of a rotational energy. The results are compared with the calculations of A.J. Sierk (*Phys. Rev.* **C33**, 2039 (1986)) on the rotating Yukawa-plus-exponential model. The heights of the fission barriers are estimated for different angular momenta in the case of the super-deformed nuclei $^{152}$Dy and $^{83}$Sr.

PACS numbers: 21.60.Ev

## 1. Introduction

Last year, at the XXIX Zakopane School of Physics, I presented our basic seven-parameter Thomas–Fermi model of macroscopic nuclear properties [3]. The model reproduces shell-corrected nuclear building energies of 1654 nuclei to within an RMS deviation of 0.655 MeV (Fig. 1), gives a good account of nuclear charge distributions (Fig. 2), fission barriers and optical model potential depths. We thought it would be interesting to see what happens when one spins up these Thomas–Fermi nuclei by adding a rotational energy $L^2/2J$, where $L$ is the angular momentum and $J$ is the moment of inertia corresponding to a common angular velocity of all mass elements. Today I will show you some recent results of these calculations.

* Presented at the "High Angular Momentum Phenomena" Workshop in honour of Zdzisław Szymański, Piaski, Poland, August 23–26, 1995.

** This work was supported by the Director, Office of Energy Research, Division of Nuclear Physics of the Office of High Energy and Nuclear Physics, of the U.S. Department of Energy under Contract No. DE-AC03-76SF00098.

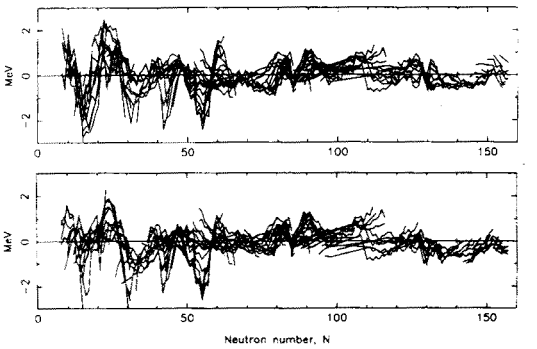


Fig. 1. The bottom part shows deviations between measured nuclear masses and the Thomas–Fermi results corrected for (Strutinsky) shell effects, an even–odd term and a semi-empirical congruence energy (Ref. [7]). The upper part is a similar plot for the shape-dependent droplet model (Ref. [12]). Lines connect isotopes of a given element.

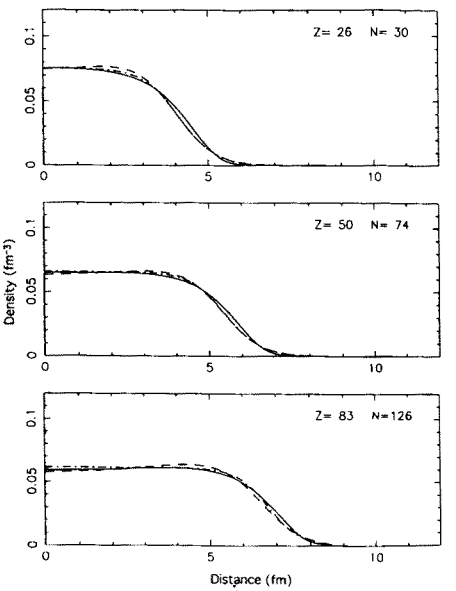


Fig. 2. The solid curves are the Thomas–Fermi charge distributions for three nuclei (with the proton size folded in). The dot-dashed and dashed curves are representations of measurements, as fitted with a Woods–Saxon function or a "three-parameter gaussian", respectively.

## 2. Comparison with A.J. Sierk's results

### *2.1. Case of L=0*

Available comprehensive studies of idealized rotating nuclei include Refs [4, 5] and, in particular, the exhaustive 1985 work of Sierk [2] on the rotating Yukawa-plus-exponential model of Krappe and Nix [6].

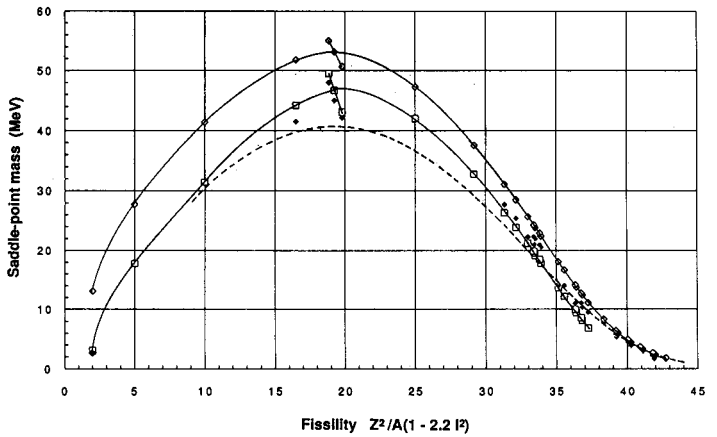


Fig. 3. Calculated and measured fission barriers from $^{8}$Be to $^{252}$Cf (corrected for ground state shell effects) as function of a fissility parameter defined as $Z^2/A(1-2.2I^2)$, where $I = (N-Z)/A$. The dashed curve refers to Sierk's calculations for nuclei on the valley of stability. The upper solid curve refers to Thomas–Fermi results which assume that the Congruence Energy is the same at the saddle point as in ground state, the lower curve that it has doubled (as expected for very necked-in shapes). The point near fissility 16 is $^{85}$Br, those near fissility 19 are $^{90,94,98}$Mo.

As a start, Fig. 3 compares fission barriers for *zero* angular momentum as calculated by Sierk (dashed curve) and according to the Thomas–Fermi model. This model predicts barriers along the upper solid curve for nuclei down to about Thorium (fissility$\sim$39), gradually drifting down towards the lower curve as the fission saddle-point shapes neck in with decreasing fissility. (The reason for the two curves has to do with the recently identified "Congruence Energy" [7]. This is an extra binding associated with the better overlap of neutron and proton densities for particles with congruent nodal structures of their wave functions. Like the shell corrections, this quantal effect is outside the framework of a Thomas–Fermi treatment, and has been represented in our model by a semi-empirical term. We have only recently figured out the approximate shape dependence of the Congruence Energy, and Fig. 3 merely shows the predictions for two limiting cases: convex (not necked-in) and very necked-in saddle-point shapes.)

You will note that for the heavy nuclei both Sierk and Thomas–Fermi agree with measurements (the solid diamonds). Then the Sierk barriers undershoot the measurements in the region of fissility 31–34. For the very light nuclei $^{85}$Br and $^{90,94,98}$Mo, Ref. [8], Sierk undershoots and Thomas–Fermi overshoots the measurements.

### *2.2. Effect of angular momentum*

The broken curves in Fig. 4 show the effect of angular momentum on the fission barriers of three nuclei studied by Sierk: $Z = 60$, 80, 100, with mass numbers chosen to lie on the valley of stability, as given by Green's formula $N - Z = 0.4\ A^2/(A + 200)$. The solid curves are the Thomas–Fermi predictions (this time with the shape dependence of the Congruence Energy taken into account). For $Z = 100$ the two predictions are again practically the same. For the lightest nucleus with $Z = 60$ Sierk's barriers are significantly below the Thomas–Fermi predictions. (The circled points correspond to the upper curve in Fig. 3, with the shape dependence of the Congruence Energy disregarded.)

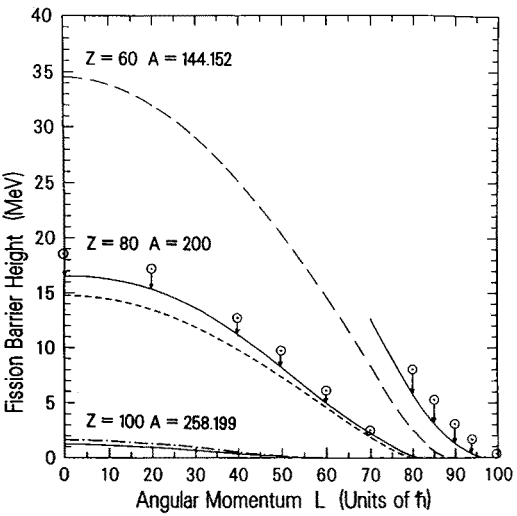


Fig. 4. Fission barriers as a function of angular momentum. The broken curves are Sierk's results from Ref. [2], the solid curves used the Thomas–Fermi model together with the shape-dependent congruence energy, and the circles show what the barriers would have been if the shape dependence had been ignored.

Sierk's calculations are considered to give a fair representation of the angular momentum dependence of fission barriers, as deduced from measurements by way of somewhat involved model dependent analyses (Ref. [9]).

By and large the same should be true of the Thomas–Fermi results. To decide whether the somewhat higher values predicted by the Thomas–Fermi model are confirmed in the case of high angular momenta (the way they are for $L = 0$ for fissility 31–34 Fig. 3) will require refined experiments and a painstaking theoretical interpretation of the results.

## 3. Fission barriers of super-deformed nuclei

Figure 5 shows the deformation energies with respect to an elongation or 'fission' coordinate in the case of $^{152}$Dy with $L = 50, 60, 70, 80, 85$ (in units of $\hbar$). The points with elongation $D = 0$ refer to the binding energies (with the rotational energy included) of the oblate Thomas–Fermi minimum-energy configurations. To explore the heights of the associated fission barriers, calculate first the distance between the centers of mass of

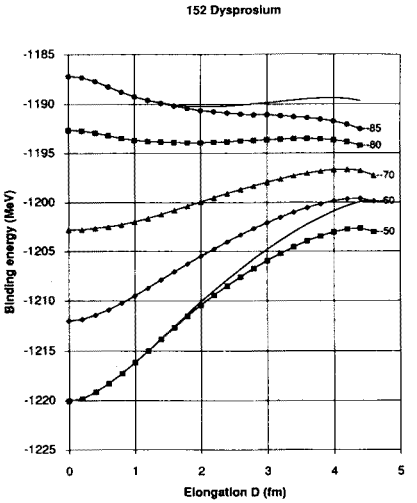


Fig. 5. The binding energy (including rotational energy) for $^{152}$Dy rotating with 50, 60, 70, 80, and 85 units of angular momentum. The "elongation" is defined as half the distance between the centers of mass of the two-halves of the triaxial shape (cut by a plane orthogonal to the longest axis), less its value for the oblate shape at $D = 0$. The two curves without symbols show the effects of ignoring the shape-dependence of the Congruence Energy.

the two halves of the oblate shape (imagined cut by a plane containing the axis of rotation). Then ask for a Thomas–Fermi solution of the rotating system, but under the constraint that this distance be greater by $2D$, with $D = 0.2$ fm, say. There results a 'stretched' triaxial shape (like a

piece of soap) rotating about the shortest axis. Repeat the calculation for $D = 04$, 0.6, 0.8... *etc.*, thus tracing out a deformation energy curve along a fission valley. A maximum along this curve will correspond to the saddle point for fission, from which the fission barrier height may be deduced. Figure 5 also illustrates the well known fact that for a sufficiently high angular momentum $\gtrsim 75$ in the case of $^{152}$Dy) a rotating macroscopic nucleus would spontaneously develop a traxial equilibrium shape. Of course, a Thomas–Fermi calculation without shell effects cannot explain the superdeformed configuration of $^{152}$, which is traxial already for much smaller values of $L$. But suppose you represent the shell correction by a narrow potential dimple, a few MeV deep, superimposed on the curves in Fig. 5 at some value $D$ of the elongation. The spacing of such curves for $\Delta L = 2$ will then correspond to the implied quadrupole $\gamma$-ray transition energies. Figure 6 shows these

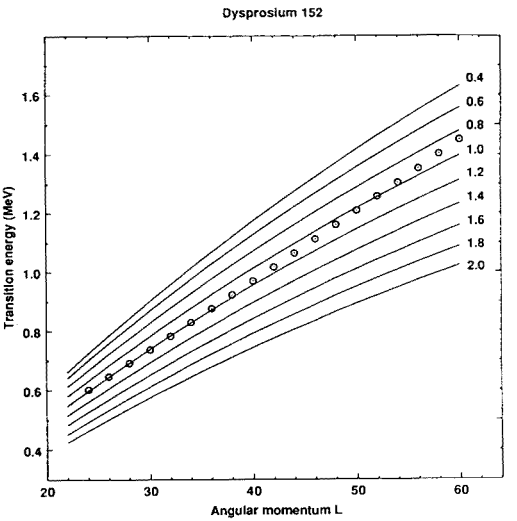


Fig. 6. The curves are quadrupole transition energies ($\Delta L = 2$) for $^{152}$Dy, calculated with the Thomas–Fermi model assuming that the elongation parameter $D$ had been frozen at the values indicated. The circles are experimental data.

energies as a function of angular momentum for different choices of $D$. For $D = 1.2$ fm one actually gets a quantitative fit to the lower part of the measured spectrum (the circled points, Ref. [10]). The subsequent deviations show that the $^{152}$Dy nucleus has a moment of inertia more nearly constant than the Thomas–Fermi model, *even when the elongation D is frozen in this model.* This is because the Thomas–Fermi nucleus is able to stretch in other degrees of freedom besides $D$ (*e.g.*, by a further flattening). By contrast, the actual Dy nucleus is pretty stiff piece of nuclear matter, with its shape frozen solid by the shell effect.

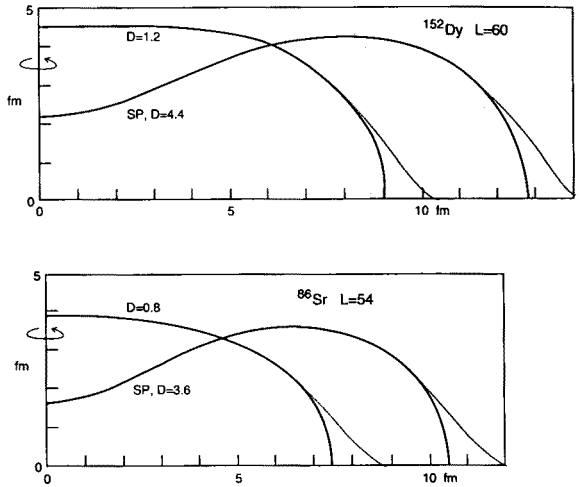


Fig. 7. The upper part shows the approximate shape of 152Dy with $L = 60$ and the elongation frozen at $D = 1.2$ fm. The corresponding saddle-point shape, for which $D$ is equal to 4.4 fm, is also shown. The lower part is the analogous plot for $^{86}$Sr with $L = 54$. The dotted curves are meant to give an impression of the diffuseness of the density distributions. The rotation axis is indicated.

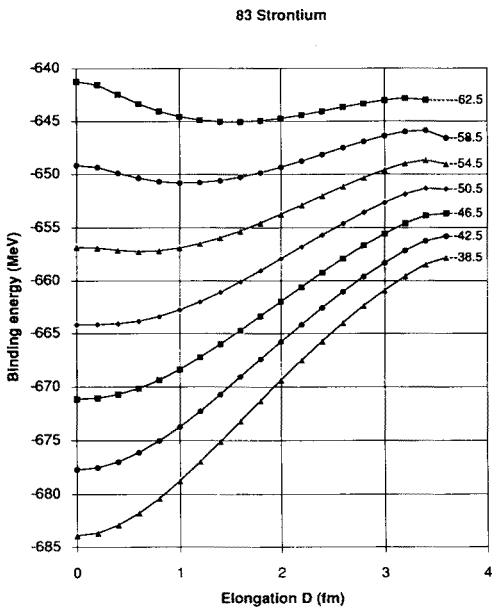


Fig. 8. This is like Fig. 5 but for $^{83}$Sr.

Figure 7 gives an indication of the shape of $^{152}$Dy with $L = 60$ for $D = 1.2$, as well as for the corresponding saddle-point shape with $D = 4.4$ (see

Fig. 5). The fission barrier height is estimated as some 13 MeV (disregarding possible shell effects at saddle point). $L \approx 60$ is the maximum angular momentum observed experimentally, and a cut-off somewhere around this value is consistent with Fig. 5, since for high $L$ the fission barrier would soon drop below the neutron binding energy and the survival probability of the system would become small.

Figures 7, 8 and 9 show a similar analysis in the case of the recently identified superdeformed band in $^{83}$Sr, with $L = 20.5 - 38.5$ (Ref. [11]).

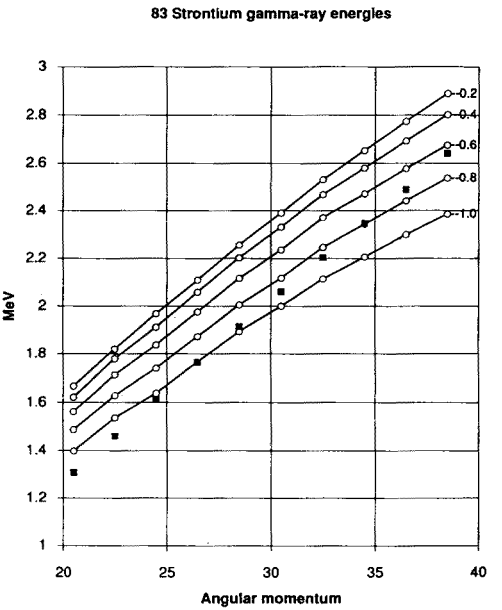


Fig. 9. This is like Fig. 6 but for $^{83}$Sr.

Figure 9 suggests a value of $D$ somewhere around $0.8 - 1.0$ fm. From Fig. 8 one estimates that at $L = 38.5$ the barrier height would be around 25 MeV, falling to about 13 MeV at $L = 50.5$. This suggests that with further experimental refinements one might be able to extend the super-deformed band in $^{83}$Sr by several units of $L$. (In the case of the heavier isotope $^{86}$Sr the Thomas–Fermi calculation estimates the fission barrier to be about 12 MeV for $L = 54$.)

## 4. Conclusions

Over the past years we have polished up a basic macroscopic model of nuclei which rests on two physical inputs: a) the 1927 semi-classical approximation of Thomas and Fermi of two fermions per $h^3$ of phase space, and

b) a seven-parameter density- and momentum-dependent effective Yukawa interaction between nucleons. The parameters have been determined by a fit to a vast database. We believe the result is a reliable description of the bulk and surface properties of the nuclear fluid, and a useful representation of what finite nuclei would look like if shell oscillations were averaged out.

It is a pleasure to dedicate this work to Zdzislaw Szymanski, who has done so much to further our understanding of *real* nuclei, as contrasted with the idealized macroscopic model nuclei with which this paper is concerned.

## REFERENCES

[1] W.D. Myers, W.J. Swiatecki, Nuclear properties according to the Thomas–Fermi model, preprint LBL-36557, December 1994, submitted to *Nucl. Phys. A*; Table of nuclear masses according to the 1994 Thomas–Fermi model, preprint LBL-36803, December 1994.
[2] A.J. Sierk, *Phys. Rev.* **C33**, 2039 (1986).
[3] W.D. Myers, W.J. Swiatecki, The nuclear Thomas–Fermi model, preprint LBL-36004, August 1994; *Acta Phys. Pol.* **B26**, 111 (1995).
[4] S. Cohen, F. Plasil, W.J. Swiatecki, *Ann. Phys.* (NY) **82**, 557 (1974).
[5] M.G. Mustafa, P.A. Baisden, H. Chandra, *Phys. Rev.* **C25**, 2524 (1992).
[6] P. Möller, J.R. Nix, *Nucl. Phys.* **A361**, 117 (1981).
[7] W.D. Myers, W.J. Swiatecki, The Congruence Energy: A contribution to nuclear masses and deformation energies, preprint LBL-37363, June 1995; Proc. Int. Conf. on Exotic Nuclei and Atomic Masses, June 19–23, 1995, Arles, France.
[8] L.G. Moretto, K.X. Jing, G.J. Wozniak, *Phys. Rev. Lett.* **74**, 3557 (1995), and private communication.
[9] F. Plasil, *Pramana-J Phys.* **33**, 145 (1989).
[10] P.J. Twin *et al.*, *Phys. Rev. Lett.* **57**, 811 (1986).
[11] D.R. LaFosse *et al.*, *Phys. Lett.* **B354**, 34 (1995).
[12] P. Möller, J.R. Nix, W.D. Myers, W.J. Swiatecki, *Atomic Data and Nuclear Data Tables* **59**, 185 (1995).